 Related Commentary, page 1222

Direct evidence for the role of caveolin-1 and caveolae in mechanotransduction and remodeling of blood vessels

Jun Yu,[1] Sonia Bergaya,[1] Takahisa Murata,[1] Ilkay F. Alp,[1] Michael P. Bauer,[1] Michelle I. Lin,[1] Marek Drab,[2] Teymuras V. Kurzchalia,[2] Radu V. Stan,[3] and William C. Sessa[1]

[1]Department of Pharmacology and Program in Vascular Cell Signaling and Therapeutics, Boyer Center for Molecular Medicine, Yale University School of Medicine, New Haven, Connecticut, USA. [2]Max Planck Institute for Molecular Cell Biology and Genetics, Dresden, Germany. [3]Department of Pathology, Dartmouth Medical School, Hanover, New Hampshire, USA.

Caveolae in endothelial cells have been implicated as plasma membrane microdomains that sense or transduce hemodynamic changes into biochemical signals that regulate vascular function. Therefore we compared long- and short-term flow-mediated mechanotransduction in vessels from WT mice, caveolin-1 knockout (*Cav-1* KO) mice, and *Cav-1* KO mice reconstituted with a transgene expressing Cav-1 specifically in endothelial cells (*Cav-1* RC mice). Arterial remodeling during chronic changes in flow and shear stress were initially examined in these mice. Ligation of the left external carotid for 14 days to lower blood flow in the common carotid artery reduced the lumen diameter of carotid arteries from WT and *Cav-1* RC mice. In *Cav-1* KO mice, the decrease in blood flow did not reduce the lumen diameter but paradoxically increased wall thickness and cellular proliferation. In addition, in isolated pressurized carotid arteries, flow-mediated dilation was markedly reduced in *Cav-1* KO arteries compared with those of WT mice. This impairment in response to flow was rescued by reconstituting Cav-1 into the endothelium. In conclusion, these results showed that endothelial Cav-1 and caveolae are necessary for both rapid and long-term mechanotransduction in intact blood vessels.

Introduction

Caveolae are described as distinct flask-shaped invaginated structures present at the surface of many cell types including endothelium (1). Contrary to the noncaveolar regions of the surface membrane, which are mainly composed of phospholipids, they have a very unique lipid composition enriched in cholesterol and sphingolipids. Among the 3 isoforms that have been described (caveolin-1 [Cav-1], Cav-2, and Cav-3), Cav-1 is the major coat protein of endothelial caveolae and is necessary for caveolae assembly. Indeed, several studies have shown a complete loss of caveolae organelles in blood vessels, adipocytes, and fibroblasts obtained from Cav-1–deficient mice (2, 3). In caveolae, Cav-1 can interact with itself to form homo-oligomers as well as with several other signaling proteins. Indeed, some intracellular signaling molecules such as the G protein α subunits, G protein–coupled receptors, receptor and nonreceptor tyrosine kinases, a number of GTPases (such as Ras and Raf), eNOS, and some components of the MAPK pathway have been described to be enriched in isolated caveolae and interact with Cav-1 (4, 5). Interestingly, several reports in the literature have shown that a large number of these signaling molecules are involved in flow/shear stress–mediated activation of endothelial cells. This suggests that Cav-1 and/or caveolae itself may serve as flow-activated mechanosensors or transducers of physiological responses in intact blood vessels.

The hypothetical role for caveolae in flow mechanosensing was first examined using a model of rat lung perfused in situ. Increasing flow and pressure in the perfused lung increased protein-tyrosine phosphorylation, eNOS activation, and coupling to the Ras/Raf/ERK MAPK pathway in a cholesterol-dependent manner (6–8). A better understanding of the mechanisms involved in flow-induced endothelial activation came from studies performed on cultured cells exposed to laminar flow in vitro. In bovine and human endothelial cells, chronic shear induced an increase in caveolae density at the luminal plasma membrane coupled with a translocation of Cav-1 from the Golgi to the plasma membrane. Chronic shear–exposed cells showed an increase in tyrosine phosphorylation of luminal surface proteins and activation of some well-known shear-sensitive signaling molecules (such as ERK, AKT, and eNOS) (9–12). In addition, it has been shown that under flow stimulation, cholesterol-disrupting drugs impaired activation of flow-sensitive proteins. Indeed, β-cyclodextrin (known to disrupt caveolae structure by depleting cholesterol content in endothelial cells) inhibited flow activation of ERK (13). Similarly, in rabbit aorta perfused ex vivo, cyclosporin A (reported to deplete cholesterol content from caveolae without disrupting their structure) decreased flow-induced phosphorylation of eNOS (at serine 1179) (14).

Despite the above findings, direct in vivo evidence supporting the role of Cav-1 during physiological arterial responses to flow is lacking. Indeed, the conclusions raised from the above experiments are mostly extrapolations of in vitro data aiming to mimic in vivo physical forces but lacking in vivo characteristics that may be relevant for mechanotransduction. First, it has been shown that the number of caveolae in cultured cells is dramatically lower compared with in vivo conditions by 80- to 1,000-fold even under flow conditions (5). Second, the cholesterol-disrupting drugs commonly used cannot distinguish cholesterol-enriched domains (called lipid rafts) from caveolae and can change membrane permeability (15, 16). Finally, and most importantly, all cultured endothelial

Nonstandard abbreviations used: Ach, acetylcholine chloride; Cav, caveolin; *Cav-1* RC, transgenic *Cav-1* KO mice reconstituted with endothelial Cav-1; LCA, left common carotid artery; LECA, left external carotid artery; L-NAME, Nω-nitro-L-arginine methyl ester hydrochloride; Phe, phenylephrine; RCA, right common carotid artery.

Conflict of interest: The authors have declared that no conflict of interest exists.

Citation for this article: *J. Clin. Invest.* **116**:1284–1291 (2006). doi:10.1172/JCI27100.

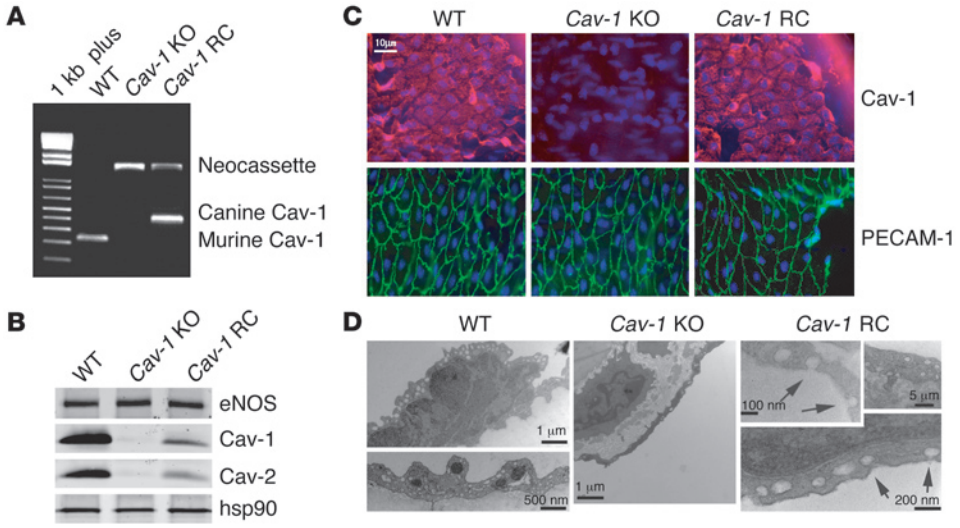

Figure 1
Characterization of carotid arteries from WT, *Cav-1* KO, and *Cav-1* RC mice. (**A**) PCR genotyping from genomic DNA extracted from tails of WT (lower band, endogenous murine Cav-1), *Cav-1* KO (upper band, neomycine cassette), and *Cav-1* RC mice (middle band, canine Cav-1 transgene). 1 kb plus, DNA Mw ladder. (**B**) Protein levels of eNOS, Cav-1, and Cav-2 in 4 pooled carotid arteries. hsp90 was used as a loading control. (**C**) In situ whole-mount immunostaining performed in WT, *Cav-1* KO, and *Cav-1* RC carotid arteries showed expression of Cav-1 protein (red) and endothelial cell marker PECAM-1 protein (green). (**D**) Representative transmission electron micrographs performed in carotid arteries from WT, *Cav-1* KO, and *Cav-1* RC mice. Arrows indicate the presence of caveolae. **C** and **D** are representative of 4 experiments.

cells are isolated from their physiological environment and therefore lacking their 3-dimensional orientation, contact with the neighboring cells, and constant exposure to the dynamically changing mechanical forces elicited by the cardiac cycle.

Thus a more definitive assessment of the role of caveolae and Cav-1 under physiological conditions using better defined tools is necessary. Therefore, the goal of our study was to use a genetic approach to determine the role of caveolae and Cav-1 in flow-mediated mechanotransduction using Cav-1 knockout (*Cav-1* KO) mice, which exhibit a complete loss of caveolae within the vessel wall, and in *Cav-1* KO mice in which endothelial Cav-1 has been reconstituted (*Cav-1* RC mice), which exhibit caveolae formation only in the endothelium. Our data document that *Cav-1* KO mice had impaired shear stress regulation of vessel diameter in vivo and in vitro, effects that were rescued by re-expression of endothelial Cav-1. These data suggest that caveolae and Cav-1 are required for short- and long-term mechanotransduction in blood vessels.

Results

Generation of transgenic mice expressing endothelial Cav-1 on a Cav-1–deficient background. As shown in Figure 1A, PCR genotyping demonstrated that WT mice expressed the endogenous murine Cav-1 gene. *Cav-1* KO mice were identified by the presence of the neomycin cassette and the absence of endogenous murine *Cav-1*. *Cav-1* KO mice bred to the endothelial-specific transgenic Cav-1 mice (17) generated *Cav-1* RC mice, which were identified by the presence of the neomycin cassette and the transgenic canine *Cav-1* gene and the lack of the endogenous murine *Cav-1* gene. Figure 1B documents protein expression in isolated carotid arteries from these mice. In all groups of mice, expression of eNOS and hsp90 were equal. In *Cav-1* KO vessels, Cav-1 and Cav-2 proteins were both absent due to the role of Cav-1 in stabilizing Cav-2 protein levels (18, 19). Interestingly, in *Cav-1* RC mice, the expression of both Cav-1 and Cav-2 was restored. The lower expression of Cav proteins observed in *Cav-1* RCs was due to the fact that Cav-1 is only re-expressed in ECs lining the vessels and that ECs are less numerous than smooth muscle cells and fibroblasts, which also express endogenous *Cav-1*. Next we used whole-mount staining of the endothelium to examine the extent of Cav-1 reconstitution in the endothelium. As shown in Figure 1C, WT and *Cav-1* RC mice had relatively equal levels of immunoreactive Cav-1 in endothelial cells as defined by the endothelial cell marker PECAM-1. *Cav-1* KO vessels lacked endothelial Cav-1 immunoreactivity without changing the levels of PECAM-1. In multiple experiments, we estimated that greater than 90% of the endothelial cells from carotid arteries, intrapulmonary arteries, and aortas were reconstituted by the transgene (data not shown). *Cav-1* KO mice lack caveolae organelles in several tissues including blood vessels, adipocytes, and fibroblasts (2, 3). As shown in Figure 1D, transmission electron micrographs documented the presence of ample caveolae in ECs lining WT carotid arteries, the loss of endothelial caveolae in *Cav-1* KO vessels, and the presence of caveolae organelles in the *Cav-1* RC vessels. These results confirmed that Cav-1 expression in endothelial cells was necessary and sufficient for caveolae formations, as previously reported (2, 3). Thus we have generated a model of endothelium-specific Cav-1 reconstitution in the *Cav-1* KO background, resulting in the formation of endothelial caveolae.

Cav-1 KO mice have impaired flow-dependent arterial remodeling in vivo and exhibit medial thickening, effects that are rescued by re-expression of endothelial Cav-1. In order to assess how changes in flow and attendant shear stress affect arterial remodeling in vivo, we ligated the external carotid artery and examined flow-dependent remodeling in the common carotid arteries of WT, *Cav-1* KO, and *Cav-1* RC mice. In this model, ligation of the left external carotid artery (LECA) resulted in a 30% decrease in flow (and shear stress) and a 10–20% decrease in lumen diameter of the left common carotid artery (LCA) — with no changes in flow and size of the contralateral carotid artery — in WT mice, as previously described by our group (20, 21). As shown in Figure 2A, ligation of the LECA for 14 days in WT mice reduced lumen diameter in the LCA by approximately 13% compared with the contralateral right common carotid artery (RCA), without any change in wall thickness (Figure 2, A and B). In contrast, ligation of the LECA in *Cav-1* KO mice did not change LCA lumen diameters but markedly increased wall thickness (by 37%) compared with RCAs. The increased wall thickness was not due to alterations in extracellular matrix, as demonstrated by the similar patterns of trichrome staining in Figure 2C. To assess the

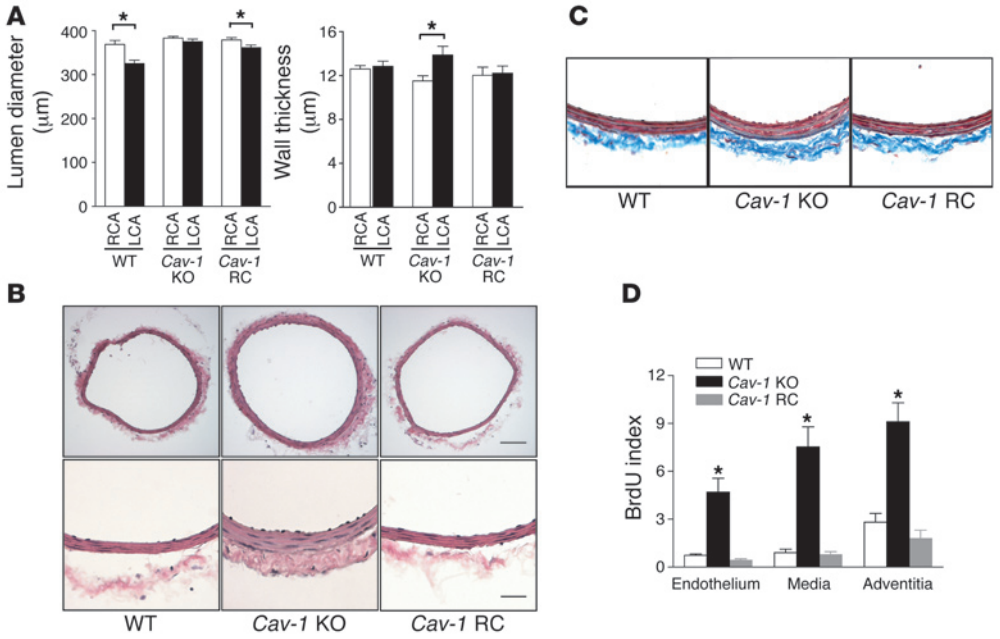

Figure 2

Cav-1 is necessary for chronic flow-induced remodeling in vivo, an effect rescued by reconstitution of Cav-1 in the endothelium. After 2 weeks of external carotid arterial ligation, morphometric analysis was performed in perfusion-fixed RCAs and LCAs from WT ($n = 6$), *Cav-1* KO ($n = 11$), and *Cav-1* RC ($n = 9$) mice. (**A**) Morphometric analysis showed a reduction in the lumen diameter of LCAs compared with contralateral RCAs in WT and *Cav-1* RC mice, with no changes in lumen diameter in *Cav-1* KO mice, in response to a reduced flow remodeling stimulus. Wall thickness remained constant in remodeled LCAs from WT and *Cav-1* RC mice, whereas wall thickness increased in LCAs of *Cav-1* KO mice. (**B** and **C**) Representative images of H&E- (**B**) or trichrome-stained (**C**) cross sections of LCAs isolated from WT, *Cav-1* KO, and *Cav-1* RC mice showed obvious increased wall thickness in remodeled *Cav-1* KO arteries. Magnification, ×400. (**D**) Increased BrdU incorporation into remodeled LCAs from *Cav-1* KO mice. Values are mean ± SEM. *$P < 0.05$, 1-way ANOVA with Bonferroni post test.

proliferation of cells during remodeling, mice of the 3 genotypes were injected with BrdU, and the BrdU labeling index was assessed. As shown in Figure 2D, the increase in wall thickness in *Cav-1* KO mice was associated with an increase in BrdU incorporation into all layers of the vessel wall. This effect was corrected in *Cav-1* RC mice, suggesting that the loss of endothelial Cav-1 increases flow-dependent proliferation and that Cav-1 is critical for mediating the ability of changes in flow to be coupled to inward remodeling in vivo. Endothelial reconstitution of Cav-1 in *Cav-1* RC mice rescued the abnormal vascular remodeling observed in *Cav-1* KO, thus allowing for a reduction in lumen diameter without significant changes in wall thickness. In conclusion, Cav-1 and endothelial caveolae were critical for arteries to sense flow changes in vivo and transduce the signals into molecular events that control lumen diameter and wall thickness (i.e., proportional vascular remodeling).

Cav-1 KO mice have impaired flow-induced vasodilation rescued by re-expression of endothelial Cav-1. It is well appreciated that another physiological readout for the actions of shear stress on blood vessel function is flow-dependent dilation. To assess whether Cav-1 is important for shear-dependent changes in vessel diameter, we examined flow-dependent dilation of carotid arteries isolated from WT, *Cav-1* KO, and *Cav-1* RC mice. Isolated carotid arteries were cannulated, set to their in vivo length, and pressurized, and responses to rapid stepwise increases in flow rate were evaluated. Since conduit arteries do not exhibit myogenic tone, vessels were preconstricted with the vasoconstrictor phenylephrine (Phe) prior to examining flow responses. In pressurized vessels, the responses to Phe were not significantly different among the 3 strains (see Methods). Under these conditions, rapid stepwise increases in intraluminal flow rates (from 0 to 800 μl/min) induced a significant increase in carotid artery lumen diameter in WT, *Cav-1* KO, and *Cav-1* RC mice reflecting flow-dependent dilation. However, these responses were markedly reduced in *Cav-1* KO arteries compared with WT arteries ($P < 0.05$, 80–800 μl/min) and were rescued by reconstitution of Cav-1 in *Cav-1* RC arteries ($P < 0.05$, 100–800 μl/min, *Cav-1* KO versus *Cav-1* RC; NS, WT versus *Cav-1* RC; Figure 3A). We also expressed the increases in lumen diameter in response to changes in flow as a function of shear stress (τ), calculated as $(4\mu Q)/(\pi r^3)$, where μ represents the viscosity coefficient; Q, the flow rate; and r, the radius of the lumen of the vessel (Figure 3B). We found that at any given shear stress, WT and *Cav-1* RC mice responded similarly, whereas *Cav-1* KO mice exhibited reduced responsiveness. Thus these data show that in vitro flow-dependent dilation of pressurized arteries was dependent on Cav-1.

Since in vitro flow-dependent dilation is known to be partially NO dependent (22–24) and Cav-1 is considered a negative regulator of eNOS function (2, 3, 25), we examined responses to another endothelium-dependent vasodilator, acetylcholine (Ach), in pressurized carotid arteries. In carotid arteries isolated from eNOS knockout mice, Ach-mediated vasodilation is absent, demonstrating that eNOS-derived NO is the major endothelial-derived relaxant in these vessels (26). As shown in Figure 3C, Ach dose-dependently increased lumen diameter to a similar extent in pressurized carotid arteries isolated from WT, *Cav-1* KO, and *Cav-1* RC mice with a trend toward greater responsiveness in *Cav-1* KO vessels. In a different preparation examining dilation of carotid arterial rings under isometric conditions, responses to Ach in WT and *Cav-1* RC carotid arteries were similar; however, Ach-induced relaxations in Cav-1 KO carotid arteries shifted leftward (Figure 3D), consistent with our hypothesis as well as previously published data (3, 4) that Cav-1 exerts an inhibitory action on eNOS. Indeed, the EC_{50}, which represents the concentration of agonist causing 50% of the maximal effect, was reduced in *Cav-1* KO carotid rings compared with WT rings (2.88×10^{-9} mol/l versus 1.16×10^{-8} mol/l, respectively). Therefore, the impaired flow-dependent dilation in *Cav-1* KO vessels is likely due to impaired shear-dependent signaling to eNOS, but not necessarily to a gross

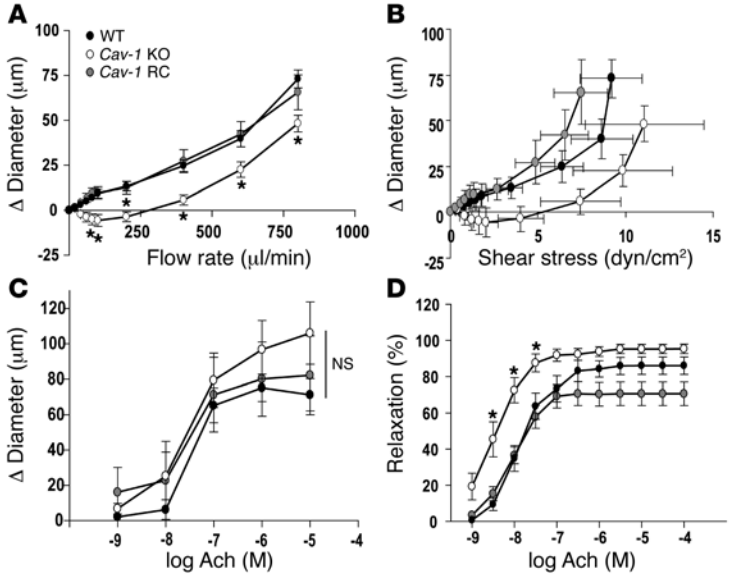

Figure 3
Cav-1 is necessary for flow-induced vasodilation, an effect rescued by reconstitution of Cav-1 in the endothelium. (**A**) Flow-induced dilations were observed in pressurized isolated carotid arteries from WT (n = 10), *Cav-1* KO (n = 8), and *Cav-1* RC mice (n = 6). Increases in lumen diameter were expressed as a function of flow rate. The flow-induced dilation was impaired in *Cav-1* KO mice compared with WT and *Cav-1* RC mice. (**B**) Increases in lumen diameter (from the same experiments as in **A**) were expressed as a function of shear stress (measured as dyn/cm^2, where 1 dyn = 1 g/cm/s^2). (**C**) Ach-induced dilations were examined after Phe contraction in pressurized isolated carotid arteries from WT (n = 6), *Cav-1* KO (n = 9), and *Cav-1* RC mice (n = 3). (**D**) Ach-induced dilations, expressed as percent relaxation of the Phe contraction, were examined in carotid rings from WT (n = 4), *Cav-1* KO (n = 4), and *Cav-1* RC mice (n = 4) mounted in a wire myograph under isometric conditions. Values are mean ± SEM. *P < 0.05, 2-way ANOVA with Bonferroni post test.

decline in eNOS function, since Ach responsiveness was normal or enhanced in carotid arteries from *Cav-1* KO mice.

Decrease of eNOS activation in response to flow in Cav-1 KO mice. The above data suggest that the loss of Cav-1 impairs flow-dependent coupling to eNOS activation. In order to assess whether the loss of Cav-1 impairs flow-dependent eNOS activation, pressurized carotid arteries from all 3 genotypes were treated with Nω-nitro-L-arginine methyl ester hydrochloride (L-NAME), and flow-induced dilation was examined. As shown in Figure 4A, L-NAME reduced flow-dependent changes in diameter in isolated WT carotid arteries. Interestingly, L-NAME did not impair flow-induced dilatation in *Cav-1* KO arteries (Figure 4B); rather, a trend toward an enhanced response to flow at higher flow rates was observed, which suggests that in the absence of Cav-1, flow-dependent coupling to eNOS is diminished in response to changes in shear stress. Similar to WT mice, L-NAME significantly reduced the response to flow in *Cav-1* RC mice (Figure 4C), demonstrating that reconstitution of Cav-1 back into the endothelium was sufficient to restore eNOS activation in response to shear stress. Comparison of the effects of L-NAME on flow-dependent responses

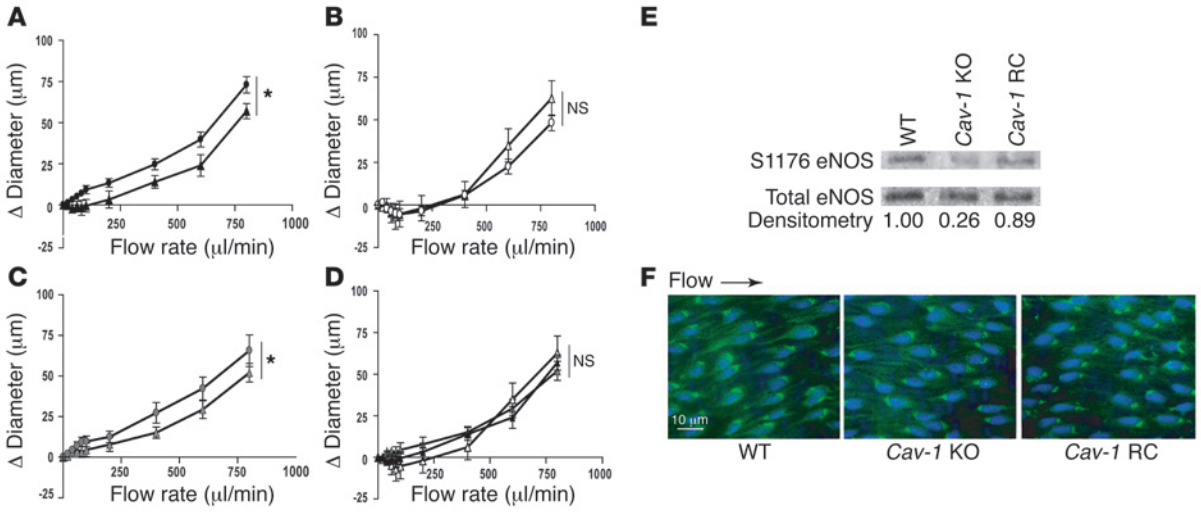

Figure 4
Cav-1 is necessary for flow-induced eNOS activation. (**A**–**D**) Flow-induced dilations in pressurized isolated carotid arteries in the absence (circles) and presence (triangles) of L-NAME from WT (**A**; filled symbols; n = 4 and 10 with and without L-NAME, respectively), *Cav-1* KO (**B**; open symbols; n = 4 and 8 with and without l-NAME, respectively), and *Cav-1* RC mice (**C**; gray symbols; n = 4 and 6 with and without l-NAME, respectively). (**D**) Comparison of flow-induced dilation performed in the presence of L-NAME between the 3 strains (n = 4 per group). The responses to flow were similar between all groups of mice in the presence of L-NAME. *P < 0.05. (**E**) Basal eNOS phosphorylation on serine 1176 was reduced in *Cav-1* KO mice and rescued in *Cav-1* RC mice. Carotid arterial lysates were prepared as described in Methods, and densitometric evaluation of the normalized ratio of phosphorylated eNOS to total eNOS is shown below. (**F**) The localization of eNOS in intact carotid arteries was similar in WT, *Cav-1* KO, and *Cav-1* RC mice. Arrow reflects the direction of flow through the vessel segment.

in carotids isolated from WT and *Cav-1* RC mice to responses in *Cav-1* KO vessels showed that the curves were superimposed (Figure 4D). Next we examined whether the phosphorylation status of eNOS on serine 1176, reflecting the in situ activation of eNOS, was different among the 3 strains (27–29). As shown in Figure 4E, Western blotting of carotid arteries from *Cav-1* KO mice revealed a reduction in basal eNOS phosphorylation on serine 1176. Endothelium-specific reconstitution of Cav-1 restored the level of phosphorylation to that seen in WT mice. Finally, we examined the subcellular localization of eNOS in isolated carotid arteries using en face imaging. As shown in Figure 4F, in WT carotid arteries, a majority of eNOS was localized in a distinct perinuclear crescent mainly downstream from the flow axis; this pattern was similar for *Cav-1* KO and *Cav-1* RC mice and consistent with previous studies examining in situ eNOS localization (30, 31).

Discussion

Shear stress is a biomechanical force generated by laminar flow on the surface of the endothelium and thought to play a major role in vascular physiology and disease. However, the mechanisms by which endothelial cells sense this mechanical stimulus and transform the signals into intracellular biochemical signals that change vessel structure and function have not been fully characterized in vivo. Caveolae and Cavs have been suspected to be involved in flow mechanosensing or transduction, based on changes in phosphorylation of resident caveolae proteins with altered pressure and flow (6–12) and in vitro experiments showing cholesterol-dependent activation of flow-mediated intracellular signaling pathways (13, 14). Thus our findings provide what we believe to be the first in vivo demonstration that endothelial cell Cav-1 and caveolae may serve as mechanosensors and/or transducers in arterial responses to changes in blood flow in intact blood vessels. We showed that flow-dependent responses in intact blood vessels required endothelial Cav-1 and caveolae, as seen by the defects in chronic flow-dependent remodeling and acute flow-dependent dilation in *Cav-1* KO mice. More importantly, reconstitution of endothelial Cav-1 into the knockout background rescued endothelial caveolae and the abnormal responsiveness of the vessels, providing clear genetic evidence supporting the role of Cav-1 in responses to flow changes in vivo.

Shear stress forces vary proportionally to flow and inversely proportionally to vessel diameter. As a consequence of this relationship, in response to long-term increases or decreases in blood flow, vessels will remodel their diameters (i.e., increase or decrease their lumen diameters, respectively) in order to normalize shear forces. In mice, rats, and rabbits, reductions in arterial diameter produced by chronic decreases in blood flow have been shown to be endothelium dependent as well as eNOS dependent (20, 21, 32, 33). In eNOS knockout mice, flow-dependent luminal remodeling is impaired and demonstrates paradoxical changes in vascular morphology, that is, no change in lumen diameter with increased wall thickness and cellularity (20). These results suggested that eNOS may act as a mechanotransducer to couple flow-activated NO release to long-term hemodynamic changes that regulate aspects of extracellular matrix turnover; endothelial and smooth muscle cell proliferation, migration, and organization; and responsiveness to growths factors necessary for adaptive remodeling. Remarkably, in the present study, chronic flow-dependent remodeling in carotid arteries from *Cav-1* KO mice phenocopied the abnormal remodeling response displayed in eNOS-deficient mice (i.e., no change in lumen diameter with an increase in wall thickness associated with increased BrdU incorporation). The increase in wall thickness and cellular proliferation in *Cav-1* KO mice is in good agreement with a recent study performed in these mice where carotid blood flow was stopped by complete ligation and a robust increase in neointima formation was shown (34). Most importantly, our data shows that the endothelium lacking caveolae was unable to couple changes in blood flow with proportional vascular remodeling, suggesting that Cav-1 or caveolae, per se, might represent an initial flow mechanosensor directly regulated by luminal blood flow. Moreover, we were able to partially correct this abnormal phenotype by reconstituting endothelial Cav-1 in the global Cav-1–deficient background. Collectively, these data strongly support the in vivo importance of the Cav-1/eNOS axis in remodeling, since mice lacking eNOS or Cav-1 develop a similar abnormal vascular remodeling phenotype in response to changes in flow and shear stress — despite the fact that in one model, eNOS is completely missing during vascular development and adulthood (*eNOS*$^{-/-}$ mice), and in the other, eNOS is present but mechanocoupling to eNOS may be impaired (*Cav-1* KO mice). A defect in coupling to eNOS in mice lacking caveolae is consistent with the recent demonstration that VEGF signaling is diminished in *Cav-1* KO mice (35).

It is appreciated that in the endothelium lining conduit vessels Cav-1 may serve as an endogenous inhibitor of eNOS function and NO production (2, 3, 5). The genetic loss of Cav-1 increases agonist-stimulated cGMP accumulation, endothelial-dependent relaxation in isolated aortae, and circulating NO levels (2, 3). Paradoxically, in the present study, we show that acute flow-dependent dilations in pressurized carotid arteries were reduced in the face of normal eNOS protein levels and normal or enhanced Ach-stimulated endothelial-dependent relaxations. Moreover, these altered responses in *Cav-1* KO vessels were corrected by re-expression of Cav-1 in the endothelium. In the perfused rat lung vasculature, a rapid increase in flow and pressure induces a rapid increase in eNOS activity, which has been shown to occur specifically in caveolar compartments. This has been correlated with the rapid dissociation of Cav-1 from the Cav-1/eNOS complex and a concomitant association of eNOS with calmodulin (7). Thus, one possible explanation for our data is that in the absence of caveolae microdomains, flow-dependent activation of lipid raft and/or caveolar-associated eNOS is reduced, leading to an impairment of flow mechanotransduction, while agonist-induced (Ach) eNOS activation (which may not require eNOS to be in caveolae; ref. 16) remains intact or actually increased due to the loss of the direct inhibitory influence of Cav-1 on eNOS. Our data showing that L-NAME diminished flow-dependent dilation in WT and *Cav-1* RC carotid arteries but was ineffective in vessels isolated from *Cav-1* KO mice strongly supports the idea that the loss of caveolae impairs flow coupling to eNOS. Moreover, basal eNOS phosphorylation on serine 1176 in mice, a key regulatory site of phosphorylation by many kinases including Akt, AMP kinase, and cAMP-dependent protein kinase, was reduced in extracts prepared from Cav-1 KO vessels, suggesting that flow activation of upstream kinases may be impaired. An alternative possible mechanism was that perhaps the loss of caveolae results in eNOS mislocalization as suggested by some (35) but not all investigators (16, 36); however, this is not the case, based on similar en face imaging of eNOS in vessels from WT, *Cav-1* KO, and *Cav-1* RC as seen in intact endothelium of humans (37) and of mice expressing the functional reporter eNOS-GFP as a transgene (30, 31).

Two very recent studies propose different mechanosensory complexes, both linked to the integrin/src/PI3K pathways, that may regulate shear signalling. One proposes that VE-cadherin, PECAM-1, and VEGFR2 constitute a mechanosensory/transducing complex in cultured endothelial cells that senses the flow upstream of integrins and transduces the signal via src/PI3K and activation of nuclear factor κB in order to promote F-actin reorganization and cell alignment (38). The role of PECAM-1 in flow sensing and flow-dependent eNOS activation and dilation has been recently reported by some (39–41) but not all (42, 43) investigators, and VEGFR2 activation is critical for shear-induced cell signalling (44) and eNOS phosphorylation (45). There are data showing that VEGFR2 can be found in caveolae and that VEGFR2 activation is impaired in endothelial cells from *Cav-1* KO mice (35), consistent with the lack of flow-dependent eNOS activation in vessels from *Cav-1* KO mice in the present study. The other study shows that inhibition of focal adhesion kinase (FAK) signaling markedly impairs flow-induced dilation as well as Akt and eNOS phosphorylation in isolated coronary arterioles (46). Given the previously described role of Cav-1 as an integral molecule involved in integrin-dependent, flow-mediated activation of FAK and actin reorganization (47, 48), the present genetic evidence supporting endothelial Cav-1 and caveolae in both acute and chronic adaptation to flow suggests that both junctional complexes (VE-cadherin and PECAM-1) and FAK most likely collaborate with resident caveolar proteins (Cav-1, VEGFR2, and eNOS) to integrate flow-dependent responses in vivo.

Methods

Mice. All animal studies were approved by the Institutional Animal Care and Use Committees of Yale University. *Cav-1* KO mice were generated by excision of exon 3 as described (2). Cav-1 heterozygous mice (F4) were intercrossed to generate litters of all 3 genotypes (WT, heterozygous, and homozygous, i.e., WT, *Cav-1*$^{+/-}$, and *Cav-1*$^{-/-}$) identified by PCR. *Cav-1* RC mice were generated by crossing transgenic mice (*Cav-1* TG) carrying canine *Cav-1* transgene under the prepro-endothelin-1 promoter expressed specifically in the endothelium (17) with *Cav-1*$^{+/-}$ mice. All mice were genotyped for the presence of endogenous murine Cav-1 (present in WT mice only; forward, 5′-TTTACCGCTTGTTGTCTACGA- 3′; reverse, 5′-TATCTCTTTCTGCGTGCTGA- 3′); the presence of the neomycin cassette (present in *Cav-1* KO and *Cav-1* RC mice; forward, 5′-TATTCTGCCTTCCTGATGATAACTG- 3′; reverse, 5′ -CCTGCGTGCAATCCATCTTGTTCAATG- 3′) and the presence of the canine *Cav-1* transgene (present in *Cav-1* RC mice only; forward, 5′ -GCAACATCTACAAGCCCAACAACA- 3′; reverse, 5′-CAGCCTCAAAGAACGGGTCACAGA- 3′). Male hybrid littermate mice (8–14 weeks old) from WT, *Cav-1* KO, or *Cav-1* RC were used in this study. Anesthesia was done by intraperitoneal injection of ketamine/xylazine (80 mg/kg ketamine, 10 mg/kg xylazine).

Western blotting. For each group of mice, 3 carotid arteries were pooled to permit detection of specific proteins. At sacrifice, mice common carotid arteries were pulverized on dry ice and then immersed in protein lysis buffer in microcentrifuge tubes and rotated for 60 minutes at 4°C. Insoluble material was removed by centrifugation at 12,000 *g* for 10 minutes at 4°C, and 35 μg protein from tissue lysates was analyzed by Western blot analysis for phosphorylated eNOS 1177, total eNOS, Cav-1, Cav-2, and hsp90 proteins.

External carotid artery ligation model. After anesthesia, mouse LECAs were ligated as previously described (20, 21). Briefly, the LECA was ligated from its origin with 7-0 nylon suture (United States Surgical). All animals were injected with BrdU subcutaneously (25 mg/kg) 3 days before sacrifice daily and intraperitoneally (30 mg/kg) 12 hours and 24 hours before death to label proliferating cells. After 14 days, mice were perfusion fixed (mean pressure of 100 mmHg with 4% paraformaldehyde in PBS, pH 7.4), and common carotid arteries were embedded in O.C.T. (Tissue-Tek; Sakura Finetek Company). Cryosections (5 μm) of arteries were obtained for H&E or elastic lamina staining. For morphometric analysis, elastin staining was performed on 10 independent cross-sections from 5 carotid arteries in each group. Cross-section images were collected using a Zeiss microscope and online charge-coupled device camera (DAGE-MTI). The circumference of internal elastic lamina (IEL) was measured, and artery diameter was calculated. The distance from IEL to external elastic lamina (EEL) in 4 locations of each section was measured by image analysis software (Scion Image Beta 4.0.2; Scion Corp.). The average was taken as wall thickness.

Histology and immunohistochemistry. For BrdU staining, arterial sections (5 μm) were quenched for endogenous peroxidase, blocked by 10% goat serum, and incubated with anti-BrdU (1:300 dilution; BD Biosciences — Pharmingen). Bound primary antibodies were detected using avidin-biotin-peroxidase (NovaRed peroxidase substrate kit; Vector Laboratories). BrdU index was the percentage of BrdU-positive cells of total nuclei in endothelium, media and adventitia. Trichrome staining was done by using Accustain Trichrome Staining kit (Sigma-Aldrich). For whole-mount staining, mouse carotid arteries were fixed with 4% paraformaldehyde (4°C, 10 min), permeabilized with 0.3% Triton-X PBS (room temperature, 30 min), and PBS containing 3% fetal bovine serum (room temperature, 30 min). The arteries were incubated with rabbit anti–Cav-1 polyclonal antibody (1:1,000 dilution; Santa Cruz Biotechnology Inc.), rat anti-PECAM polyclonal antibody (1:400 dilution; BD Biosciences), and anti-eNOS monoclonal antibody (1:300 dilution; BD). Alexa 568 anti-rabbit IgG and 488 anti-rat IgG (Invitrogen Corp.) were used as secondary antibodies (1:200 dilution, room temperature, 1 hr).

Pressurized and perfused isolated carotid arteries. Midsternal thoracotomy was performed, and LCAs and RCAs were carefully exposed and quickly excised. Blinded experiments were performed using WT, *Cav-1* KO, and *Cav-1* RC carotid arteries, which were then mounted in vitro in an arteriograph, where flow and pressure can be modified independently, as described previously (22, 23). Briefly, the carotid artery was cannulated at both extremities and placed in a bath containing a modified Krebs-Ringer solution (118.3 mmol/l NaCl, 5.5 mmol/l glucose, 4.7 mmol/l KCl, 2.5 mmol/l $CaCl_2$, 1.2 mmol/l KH_2PO_4, 1.2 mmol/l $MgSO_4$, 25 mmol/l $NaHCO_3$, and 5 mmol/l HEPES, pH 7.4) at 37°C and gassed with a mixture of 95% O_2/5% CO_2. Intraluminal and extraluminal perfusions were provided by 2 perfusion pumps. The carotid artery was maintained under a transmural pressure of 70 mmHg throughout the experiments. The internal diameters were determined with a binocular loop (Model XC-73; Sony Corp.) connected to a video camera system (Living System Instrumentation Inc.). The pressure at both ends of the artery was monitored using 2 pressure transducers (P1 and P2) placed at equal distances from the vessel. Therefore, the mean pressure calculated from P1 and P2 pressures can be assumed to be representative of the lumen pressure of the artery. Furthermore, during flow increases experiments (from 0 to 800 μl/min), intraluminal pressure was maintained using a pressure servo-control (Living System Instrumentation Inc.) connected downstream of the vessel, so that flow could be increased without significant changes in pressure. The difference in pressure (P1 – P2) recorded at the maximal flow rate imposed to the vessel (800 μl/min) in *Cav-1* KO and *Cav-1* RC mice were similar to the WT group of mice (11.6 ± 0.7 mmHg, 10.9 ± 0.4 mmHg, and 13.5 ± 1.2 mmHg; P = NS). The lumen diameter of the artery, as well as the upstream (P1) and downstream (P2) pressures, were continuously recorded using Chart software (version 4.2 for Windows; ADInstruments) software. At the beginning of each experiment, vessels were equilibrated for 40 minutes at 70 mmHg with no flow rate intraluminally. The pres-

ence of a functional endothelium was evaluated by assessing the relaxation by Ach (1 μmol/l; Sigma-Aldrich) during L-Phe hydrochloride–induced contraction (1 μmol/l; Sigma-Aldrich). All the experiments included in further analysis showed a relaxation by Ach greater than 70%, revealing that the endothelial layer was not damaged.

Responses to step increases in flow rate (from 0 to 800 μl/min) were evaluated during contraction to Phe (present intraluminally and extraluminally), as carotid arteries do not develop myogenic tone. We matched Phe contractions with the WT group of mice (–81 ± 11 μm [n = 10], –108 ± 14 μm [n = 8], and –53 ± 5 μm [n = 6] in WT, *Cav-1* KO, and *Cav-1* RC mice, respectively; P = NS, WT versus *Cav-1* KO and *Cav-1* RC).

In a separate set of experiments, we assessed the effects of L-NAME (100 μmol/l; Sigma-Aldrich) on the responses to flow in WT, *Cav-1* KO, and *Cav-1* RC mice (n = 4 per group), again during precontraction with Phe. The change in pressure recorded at the maximal flow rate imposed to the vessel (800 μl/min) in WT and *Cav-1* RC mice were similar to the *Cav-1* KO group of mice (14.7 ± 0.8 mmHg, 10.2 ± 0.7 mmHg, and 12.1 ± 0.6 mmHg, respectively; P = NS). After verification of the integrity of the endothelial layer as described above, L-NAME and Phe were incubated simultaneously intraluminally and extraluminally for 45 minutes, and step increases in flow rates were performed similarly to the above-mentioned control conditions (Phe without L-NAME). We matched the contractions reached in presence of Phe plus L-NAME between both groups of mice (WT, –158 ± 35 μm; *Cav-1* KO, –155 ± 47 μm; *Cav-1* RC, –158 ± 37 μm; n = 4 per group; P = NS between WT, *Cav-1* KO, and *Cav-1* RC).

Responses to Ach (from 10^{-9} to 10^{-5} M) were also examined in this system after precontraction with Phe. Again, we matched the Phe-induced contractions with the WT group of mice (WT, –78 ± 6 μm [n = 6]; *Cav-1* KO, –114 ± 16 μm [n = 9]; *Cav-1* RC, –70 ± 13 μm [n = 3]; P = NS, WT versus *Cav-1* KO and *Cav-1* RC).

Carotid arterial ring studies. Carotid arteries from WT, *Cav-1* KO, and *Cav-1* RC mice were cut into 2-mm-long rings. Rings were suspended by 2 tungsten wires mounted in a vessel myograph system (Danish Myo Technology A/S). Carotid rings were bathed in oxygenated Krebs buffer (119 mmol/l NaCl, 11 mmol/l glucose, 4.2 mmol/l KCl, 2.5 mmol/l $CaCl_2$, 1.2 mmol/l KH_2PO_4, 1.2 mmol/l $MgSO_4$, 25 mmol/l $NaHCO_3$, 0.026 mmol/l EDTA) and submitted to a resting tension of 5 mN. After 30 minutes of equilibration with frequent washings, concentration response curves for Phe were generated to determine vasoconstrictor responses. To study vasodilator responses, rings were preconstricted with a concentration of Phe corresponding to the EC_{50-70}, and dilations to Ach (from 10^{-9} to 10^{-5} M) were examined.

Statistics. All data are expressed as mean ± SEM. In in vitro studies, data are given as change in diameter (μm) or tension relaxation (%). Statistical evaluation was performed using either 1-way or 2-way ANOVA for repeated measures followed by a Bonferonni post test. In in vivo studies, statistical evaluation was performed by use of ANOVA for repeated measures followed by Bonferroni post test. A value of $P < 0.05$ was considered statistically significant.

Acknowledgments

This work was supported by NIH grants R01 HL64793, RO1 HL 61371, R01 HL 57665, and PO1 HL 70295 to W.C. Sessa and a postdoctoral grant from the French "Ministère des Affaires Etrangères" (Bourse lavoisier-programme général, Egide) and the Fundation "Simone et Cino Del Duca" (France) to S. Bergaya.

Received for publication October 11, 2005, and accepted in revised form January 17, 2006.

Address correspondence to: William C. Sessa, Department of Pharmacology and Program in Vascular Cell Signaling and Therapeutics, Boyer Center for Molecular Medicine, Yale University School of Medicine, New Haven, Connecticut 06536, USA. Phone: (203) 737-2213; Fax: (203) 737-2290; E-mail: william.sessa@yale.edu.

Jun Yu and Sonia Bergaya contributed equally to this work.

1. Bruns, R.R., and Palade, G.E. 1968. Studies on blood capillaries. I. General organization of blood capillaries in muscle. *J. Cell Biol.* **37**:244–276.
2. Drab, M., et al. 2001. Loss of caveolae, vascular dysfunction, and pulmonary defects in caveolin-1 gene-disrupted mice. *Science.* **293**:2449–2452.
3. Razani, B., et al. 2001. Caveolin-1 null mice are viable but show evidence of hyperproliferative and vascular abnormalities. *J. Biol. Chem.* **276**:38121–38138.
4. Smart, E.J., et al. 1999. Caveolins, liquid-ordered domains, and signal transduction. *Mol. Cell. Biol.* **19**:7289–7304.
5. Gratton, J.P., Bernatchez, P., and Sessa, W.C. 2004. Caveolae and caveolins in the cardiovascular system. *Circ. Res.* **94**:1408–1417.
6. Schnitzer, J.E., Oh, P., Jacobson, B.S., and Dvorak, A.M. 1995. Caveolae from luminal plasmalemma of rat lung endothelium: microdomains enriched in caveolin, Ca(2+)-ATPase, and inositol trisphosphate receptor. *Proc. Natl. Acad. Sci. U. S. A.* **92**:1759–1763.
7. Rizzo, V., McIntosh, D.P., Oh, P., and Schnitzer, J.E. 1998. In situ flow activates endothelial nitric oxide synthase in luminal caveolae of endothelium with rapid caveolin dissociation and calmodulin association. *J. Biol. Chem.* **273**:34724–34729.
8. Rizzo, V., Sung, A., Oh, P., and Schnitzer, J.E. 1998. Rapid mechanotransduction in situ at the luminal cell surface of vascular endothelium and its caveolae. *J. Biol. Chem.* **273**:26323–26329.
9. Boyd, N.L., et al. 2003. Chronic shear induces caveolae formation and alters ERK and Akt responses in endothelial cells. *Am. J. Physiol. Heart Circ. Physiol.* **285**:H1113–H1122.
10. Rizzo, V., Morton, C., DePaola, N., Schnitzer, J.E., and Davies, P.F. 2003. Recruitment of endothelial caveolae into mechanotransduction pathways by flow conditioning in vitro. *Am. J. Physiol. Heart Circ. Physiol.* **285**:H1720–H1729.
11. Sun, R.J., Muller, S., Stoltz, J.F., and Wang, X. 2002. Shear stress induces caveolin-1 translocation in cultured endothelial cells. *Eur. Biophys. J.* **30**:605–611.
12. Sun, R.J., Muller, S., Zhuang, F.Y., Stoltz, J.F., and Wang, X. 2003. Caveolin-1 redistribution in human endothelial cells induced by laminar flow and cytokine. *Biorheology.* **40**:31–39.
13. Park, H., et al. 1998. Plasma membrane cholesterol is a key molecule in shear stress-dependent activation of extracellular signal-regulated kinase. *J. Biol. Chem.* **273**:32304–32311.
14. Lungu, A.O., et al. 2004. Cyclosporin A inhibits flow-mediated activation of endothelial nitric-oxide synthase by altering cholesterol content in caveolae. *J. Biol. Chem.* **279**:48794–48800.
15. Munro, S. 2003. Lipid rafts: elusive or illusive? *Cell.* **115**:377–388.
16. Sowa, G., Pypaert, M., and Sessa, W.C. 2001. Distinction between signaling mechanisms in lipid rafts vs. caveolae. *Proc. Natl. Acad. Sci. U. S. A.* **98**:14072–14077.
17. Bauer, P.M., et al. 2005. Endothelial-specific expression of caveolin-1 impairs microvascular permeability and angiogenesis. *Proc. Natl. Acad. Sci. U. S. A.* **102**:204–209.
18. Mora, R., et al. 1999. Caveolin-2 localizes to the golgi complex but redistributes to plasma membrane, caveolae, and rafts when co-expressed with caveolin-1. *J. Biol. Chem.* **274**:25708–25717.
19. Parolini, I., et al. 1999. Expression of caveolin-1 is required for the transport of caveolin-2 to the plasma membrane. Retention of caveolin-2 at the level of the golgi complex. *J. Biol. Chem.* **274**:25718–25725.
20. Rudic, R.D., et al. 1998. Direct evidence for the importance of endothelium-derived nitric oxide in vascular remodeling. *J. Clin. Invest.* **101**:731–736.
21. Rudic, R.D., Bucci, M., Fulton, D., Segal, S.S., and Sessa, W.C. 2000. Temporal events underlying arterial remodeling after chronic flow reduction in mice: correlation of structural changes with a deficit in basal nitric oxide synthesis. *Circ. Res.* **86**:1160–1166.
22. Bergaya, S., et al. 2001. Decreased flow-dependent dilation in carotid arteries of tissue kallikrein-knockout mice. *Circ. Res.* **88**:593–599.
23. Bergaya, S., et al. 2004. Flow-dependent dilation mediated by endogenous kinins requires angiotensin AT2 receptors. *Circ. Res.* **94**:1623–1629.
24. Vequaud, P., and Freslon, J.L. 1996. Components of flow-induced dilation in rat perfused coronary artery. *Cell Biol. Toxicol.* **12**:227–232.
25. Bucci, M., et al. 2000. In vivo delivery of the caveolin-1 scaffolding domain inhibits nitric oxide synthesis and reduces inflammation. *Nat. Med.* **6**:1362–1367.
26. Scotland, R.S., et al. 2002. Functional reconstitution of endothelial nitric oxide synthase reveals the importance of serine 1179 in endothelium-dependent vasomotion. *Circ. Res.* **90**:904–910.
27. Dimmeler, S., et al. 1999. Activation of nitric oxide synthase in endothelial cells by Akt-dependent phosphorylation. *Nature.* **399**:601–605.
28. Fulton, D., et al. 1999. Regulation of endothelium-

derived nitric oxide production by the protein kinase Akt. *Nature.* **399**:597–601.
29. Dixit, M., et al. 2005. Gab1, SHP2, and protein kinase A are crucial for the activation of the endothelial NO synthase by fluid shear stress. *Circ. Res.* **97**:1236–1244.
30. van Haperen, R., et al. 2003. Functional expression of endothelial nitric oxide synthase fused to green fluorescent protein in transgenic mice. *Am. J. Pathol.* **163**:1677–1686.
31. Cheng, C., et al. 2005. Shear stress affects the intracellular distribution of eNOS: direct demonstration by a novel in vivo technique. *Blood.* **106**:3691–3698.
32. Guyton, J.R., and Hartley, C.J. 1985. Flow restriction of one carotid artery in juvenile rats inhibits its growth of arterial diameter. *Am. J. Physiol.* **248**:H540–H546.
33. Langille, B.L., and O'Donnell, F. 1986. Reductions in arterial diameter produced by chronic decreases in blood flow are endothelium-dependent. *Science.* **231**:405–407.
34. Hassan, G.S., Jasmin, J.F., Schubert, W., Frank, P.G., and Lisanti, M.P. 2004. Caveolin-1 deficiency stimulates neointima formation during vascular injury. *Biochemistry.* **43**:8312–8321.
35. Sonveaux, P., et al. 2004. Caveolin-1 expression is critical for vascular endothelial growth factor-induced ischemic hindlimb collateralization and nitric oxide-mediated angiogenesis. *Circ. Res.* **95**:154–161.
36. Gonzalez, E., Nagiel, A., Lin, A.J., Golan, D.E., and Michel, T. 2004. Small interfering RNA-mediated down-regulation of caveolin-1 differentially modulates signaling pathways in endothelial cells. *J. Biol. Chem.* **279**:40659–40669.
37. Sessa, W.C., et al. 1995. The Golgi association of endothelial nitric oxide synthase is necessary for the efficient synthesis of nitric oxide. *J. Biol. Chem.* **270**:17641–17644.
38. Tzima, E., et al. 2005. A mechanosensory complex that mediates the endothelial cell response to fluid shear stress. *Nature.* **437**:426–431.
39. Dusserre, N., et al. 2004. PECAM-1 interacts with nitric oxide synthase in human endothelial cells: implication for flow-induced nitric oxide synthase activation. *Arterioscler. Thromb. Vasc. Biol.* **24**:1796–1802.
40. Osawa, M., Masuda, M., Kusano, K., and Fujiwara, K. 2002. Evidence for a role of platelet endothelial cell adhesion molecule-1 in endothelial cell mechanosignal transduction:is it a mechanoresponsive molecule? *J. Cell Biol.* **158**:773–785.
41. Bagi, Z., et al. 2005. PECAM-1 mediates NO-dependent dilation of arterioles to high temporal gradients of shear stress. *Arterioscler. Thromb. Vasc. Biol.* **25**:1590–1595.
42. Kaufman, D.A., Albelda, S.M., Sun, J., and Davies, P.F. 2004. Role of lateral cell-cell border location and extracellular/transmembrane domains in PECAM/CD31 mechanosensation. *Biochem. Biophys. Res. Commun.* **320**:1076–1081.
43. Sumpio, B.E., et al. 2005. MAPKs (ERK1/2, p38) and AKT can be phosphorylated by shear stress independently of platelet endothelial cell adhesion molecule-1 (CD31) in vascular endothelial cells. *J. Biol. Chem.* **280**:11185–11191.
44. Wang, Y., et al. 2002. Interplay between integrins and FLK-1 in shear stress-induced signaling. *Am. J. Physiol. Cell Physiol.* **283**:C1540–C1547.
45. Jin, Z.G., Wong, C., Wu, J., and Berk, B.C. 2005. Flow shear stress stimulates Gab1 tyrosine phosphorylation to mediate protein kinase B and endothelial nitric-oxide synthase activation in endothelial cells. *J. Biol. Chem.* **280**:12305–12309.
46. Koshida, R., et al. 2005. Role of focal adhesion kinase in flow-induced dilation of coronary arterioles. *Arterioscler. Thromb. Vasc. Biol.* **25**:2548–2553.
47. Wei, Y., Yang, X., Liu, Q., Wilkins, J.A., and Chapman, H.A. 1999. A role for caveolin and the urokinase receptor in integrin-mediated adhesion and signaling. *J. Cell Biol.* **144**:1285–1294.
48. Radel, C., and Rizzo, V. 2005. Integrin mechanotransduction stimulates caveolin-1 phosphorylation and recruitment of Csk to mediate actin reorganization. *Am. J. Physiol. Heart Circ. Physiol.* **288**:H936–H945.